AD-A009 958

ANAYLSIS OF CONTROLLER/SYSTEM DYNAMICS FOR A REMOTELY PILOTED VEHICLE STRIKE MISSION

Anil Phatak, et al

Systems Control, Incorporated

Prepared for:

Aerospace Medical Research Laboratory

May 1975

Unclassified

SECURITY CLASSIFICATION OF THIS PAGE (When Data Entered)

REPORT DOCUMENTATION PAGE		READ INSTRUCTIONS BEFORE COMPLETING FORM
1. REPORT NUMBER AMRL TR-74-80	2. GOVT ACCESSION NO.	3. RECIPIENT'S CATALOG NUMBER AD-A009958
4. TITLE (and Subtitle) ANALYSIS OF CONTROLLER/SYSTEM DYNAMICS FOR A REMOTELY PILOTED VEHICLE STRIKE MISSION		5. TYPE OF REPORT & PERIOD COVERED Final Report 6. PERFORMING ORG. REPORT NUMBER
7. AUTHOR(s) Anil Phatak, Narendra Gupta, Ilana Segall		8. CONTRACT OR GRANT NUMBER(s) F33615-73-C-4021
9. PERFORMING ORGANIZATION NAME AND ADDRESS Systems Control, Inc. 1801 Page Mill Road Palo Alto, California 94304		10. PROGRAM ELEMENT, PROJECT, TASK AREA & WORK UNIT NUMBERS 62202F, 7222-09-12
11. CONTROLLING OFFICE NAME AND ADDRESS Aerospace Medical Research Laboratory, Aerospace Medical Division, Air Force Systems Command, Wright-Patterson Air Force Base, Ohio 45433		12. REPORT DATE May 1975 13. NUMBER OF PAGES ~~55~~ 54
14. MONITORING AGENCY NAME & ADDRESS(if different from Controlling Office)		15. SECURITY CLASS. (of this report) Unclassified 15a. DECLASSIFICATION/DOWNGRADING SCHEDULE

16. DISTRIBUTION STATEMENT (of this Report)

Approved for public release; distribution unlimited

17. DISTRIBUTION STATEMENT (of the abstract entered in Block 20, if different from Report)

18. SUPPLEMENTARY NOTES

19. KEY WORDS (Continue on reverse side if necessary and identify by block number)

covariance propagation
aircraft dynamics
human operator
optimal control models
remotely piloted vehicle (XQM-103)
performance
strike mission
weapon delivery
general purpose bomb
fixed depressed reticle sight

20. ABSTRACT (Continue on reverse side if necessary and identify by block number)

This report presents an approach for evaluating various subsystems of a remotely piloted vehicle (RPV) during a strike mission. Specific consideration is given to the three mission phases of weapon delivery, takeoff and landing. The air-to-ground weapon delivery task assumes the use of a general purpose bomb and a fixed depressed reticle sight. The weapon delivery profile is divided into three segments: (1) target acquisition to arrival at the launch point for initiation of attack; (2) launch point to weapon release point; and

DD FORM 1 JAN 73 1473 EDITION OF 1 NOV 65 IS OBSOLETE

SECURITY CLASSIFICATION OF THIS PAGE (When Data Entered)

20. (3) weapon release point to bomb impact point. Error covariance propagation methods are used to relate bomb impact errors to errors in the flight condition at the weapon release point, and to relate weapon release point errors to piloting errors from attack initiation to weapon release. The remote pilot is assumed to behave as an optimal controller and state estimator and, therefore, described by the optimal control model for the human operator. This report demonstrates the usefulness of pilot/vehicle modeling as an effective tool in the analysis and design of a RPV strike mission by isolating the prime sources of piloting and system degradations in terms of their effects on weapon delivery performance. Insight gained from such studies should prove valuable for recommending system improvements through modifications in the displays, vehicle augmentation, and the overall weapon delivery profile. Finally, the methodology developed in this report should be applicable in determining the limitations of remote human controllers with regard to their ability to fly one or more RPV's under varying levels of system degradation (e.g., downlink jamming).

PREFACE

This research was done under Contract F33615-73-C-4021 by Systems Control, Inc., Palo Alto, California for the 6570th Aerospace Medical Research Laboratory, Wright-Patterson Air Force Base, Ohio in support of Project 0100. The Air Force project monitor on this contract was Dr. Carroll Day. At SCI, the project manager and principal investigator was Anil Phatak. Narendra Gupta was the project engineer. Ilana Segall was the programmer/analyst. Technical discussions with Jayant Karmarkar of SCI are acknowledged.

This work was supported in part
under the Laboratory Commanders Fund

TABLE OF CONTENTS

LIST OF FIGURES

LIST OF TABLES

INTRODUCTION

The development of an analytical model for the remote human controller/vehicle dynamics during the critical phases of a remotely piloted vehicle (RPV) strike mission is a prerequisite for the quantitiative understanding and evaluation of the overall mission effectiveness. The purpose of this report is to develop such a modeling approach and demonstrate its usefulness as an effective tool in the design of a baseline RPV strike mission. Analysis of the controller/vehicle dynamics is used to isolate the principal causes of degradations in the overall weapon system effectiveness. Insight gained from these analyses should prove extremely valuable in selecting a baseline configuration including specific recommentations for the choice of displays, the vehicle augmentation, and the overall RPV strike mission flight profile.

Primary consideration is given in this report to the three mission phases of Takeoff, Landing and Weapon Delivery. A general description of the RPV strike mission is given followed by a detailed analysis of the weapon delivery and Takeoff and Landing segments of the strike profile. An appendix is included on the design of a command director for the weapon delivery phase.

THE RPV STRIKE MISSION

The principal subsystems of an RPV system are:

1. The vehicle.

2. The navigation and autopilot.

3. The onboard vehicle sensors.

4. The two-way communications or data link between the RPV and the human operator in a remote station.

5. The human operator who controls and communicates with the RPV.

6. The central control center and one or more relay aircraft.

An RPV system by its very definition implies that a vehicle must be remotely controlled by a human operator (i.e., a pilot, a weapons controller or an air traffic controller, for example) so as to satisfy the prescribed mission requirements. Thus, the design of a specific RPV system can range from a completely manual mode of operation where the operator would be totally responsible for control and guidance of the vehicle(s) to a fully automatic mode where the vehicle(s) would be autonomous and preprogrammed for the given mission requirements. However, both of the above two extremes in design can be recognized as impractical if not infeasible. A reasonable design, therefore, is a semiautomatic system, where a tradeoff must be made in the functions allocated to automation and to man. The selection of a specific baseline configuration would obviously be dependent on the constraints imposed by the individual RPV subsystems and, in particular, on the onboard computers, image sensors and the two-way data link between the vehicle and the remote operator. What is rquired, therefore, is a systematic approach to the design of a baseline system for an RPV strike mission. This report presents an analytical approach to determining the optimum operator/RPV interface.

OPERATIONAL PHASES: HUMAN OPERATOR CONSIDERATIONS

The overall strike mission may be partitioned into nine individual operational phases. They are:

1. Takeoff
2. Climb

} Launch

3. Enroute Navigation
4. Target Acquisition
5. Weapon Delivery
6. Target Damage Assessment
7. Return Route Navigation
8. Approach
9. Landing

} Recovery

A design of a baseline system involves the allocation of tasks to the remote pilot or to automation. It is reasonable to assume that the remote controller would be primarily involved in all of the above phases except enroute and return route navigation. During these phases, the human operator must perform control tasks corresponding to closed-loop tracking, regulation and open-loop command generation, and decision tasks of target detection, discrimination, and identification (or recognition).

The discussion in this report is limited to the analysis of the remote controller/RPV interface for the three phases of takeoff, landing and weapon delivery. The weapon delivery task is the most demanding of the remote controller and is, therefore, analyzed in greater detail than the takeoff and landing tasks. Detailed discussion of these three tasks follows.

THE MANUAL WEAPON DELIVERY TASK

The manual weapon delivery task begins immediately following target detection and acquisition and requires that the remote pilot initiate attack and fly a suitable weapon delivery profile until release of the bomb at some preselected nominal flight condition. The overall weapon delivery profile can conveniently be partitioned into three segments as follows:

1. Target acquisition to arrival at launch point for initiation of attack;

2. Launch point to weapon release point; and

3. Weapon release point to bomb impact point.

Following decision to initiate attack, the human operator must typically maneuver (i.e., dive and roll) the aircraft so as to arrive at the preselected nominal weapon release flight condition. It is assumed here that the only flight variables displayed to the pilot are the aircraft's attitude (pitch, yaw, and roll), airspeed, altitude, angle-of-attack, and sideslip angle.

A depressed reticle optical sight superimposed on a TV monitor (video, infrared, or radar) for the target area is the only display for target tracking during air-to-ground bomb delivery. In dive bombing with a conventional bomb, the bomb velocity vector at the instant of nominal weapon release (also called pickle point) is the same as that of the aircraft. However, the bomb trajectory impacts short of the point predicted by a rectilinear trajectory along the initial velocity vector because of the effects of gravity and aerodynamic drag. Thus, the reticle image must be depressed below the fuselage longitudinal axis by an angle, whose magnitude is dependent on the nominal weapon release flight condition (i.e., nominal weapon release attitude, angle-of-attack, altitude, and airspeed). Therefore, to score a direct hit on the target, the remote pilot must maneuver the RPV from the initial conditions at launch point so as to arrive at the pickle point with the pipper on target and the aircraft altitude, dive angle and airspeed at the preselected nominal values. For the purpose of this discussion, the aircraft is assumed to be programmed for coordinated turns; hence, elevator

and ailerons are the only two control commands available to the remote operator. The throttle command is assumed to have been set prior to initiation of attack so as to give a preselected nominal airspeed at launch point. A pilot (remote or onboard) can perform this complex multivariable task only after several hours of training in-flight or on simulators. Even though details in piloting techniques are bound to vary between different pilots, the rudimentary procedures are likely to be common across the population and may be summarized as follows:

1. Acquire the target on the TV monitor.

2. Decide on the launch flight condition at the initiation of attack. For example, attack must be launched when aircraft attitude (pitch and roll angles), angle-of-attack, airspeed, altitude and target range (or equivalently the position of the pipper relative to the target) are at some preselected launch flight condition. Usually, the roll attitude at launch is selected as zero (wings level) while the dive angle at launch depends upon the nominal weapon delivery profile selected by a given operator. As a result, the human pilot corrects for the azimuth and roll errors prior to launch point primarily by using aileron commands. Hence, the nominal weapon delivery profile from launch to weapon release can be restricted to the vertical plane and requires primarily longitudinal control commands through the elevator; the aileron being used for gust alleviation alone.

3. Having maneuvered the aircraft to the preselected launch flight condition, begin attack by applying learned nominal elevator command to achieve desired nominal weapon delivery profile to pickle point. This learned elevator command is what is referred to as precognitive (open-loop or feedforward) control on behalf of the pilot.

4. Perform compensatory tracking to minimize the effects of gust disturbances on the desired nominal trajectory. This would require the use of elevator and aileron deflections from the nominal command inputs to compensate for longitudinal and lateral tracking errors from the nominal flight profile.

5. Release weapon when aircraft flight conditions are closest to the pre-selected release criteria and with the pipper on target.

6. Follow some optimal evasive escape profile to return the RPV to the next phase of the overall mission.

Differences in flying technique are most likely to occur in the a priori learned selection of the launch initial conditions and the subsequent choice of a nominal precognitive elevator command input. For example, it is well known that onboard pilots of fighter aircraft such as the F-4 prefer a hyperbolic longitudinal attack profile with steep dive angles at initiation of attack which get shallower as the pickle point is reached. There are several reasons why fighter pilots may prefer such maneuvers. Most obvious are: (1) the pilots prefer +ve g_z over -ve g_z forces, (2) target range estimates may be continually obtained as long as pipper is not on target, (3) a hyperbolic flight profile may be optimal from the point of energy (or fuel) management, and, finally, (4) the escape profile may be safer by being farther from the target area and at the same time impose smaller +ve g_z forces on the pilot.

No such restrictions are necessary for the RPV weapon delivery task because the pilot is not onboard the aircraft. It is reasonable, therefore, to consider other flying techniques in training a remote pilot for a tactical RPV weapon delivery task. An important criterion in the selection of a flying technique for RPV operators should be the simplicity of the procedure and the ability to quickly train novice operators instead of highly skilled fighter pilots.

ERROR ANALYSIS OF THE WEAPON DELIVERY PHASE

The two separate segments of the weapon delivery profile corresponding to post and pre-weapon release are analyzed in detail in the following. The principal aim of the analyses is, first, to relate the bomb impact errors to errors in the flight conditions at pickle point; second, to relate the pickle point errors to piloting errors from attack initiation to weapon release; and third, to show the usefulness of error propagation and human operator models as design tools for RPV systems.

Post-Weapon Release (Free Fall)

During this phase, the bomb falls under the influence of gravity and aerodynamic forces. The air resistance of most bombs is fairly small and, therefore, small changes in the windspeed or the bomb velocity from its nominal value produce small changes in aerodynamic drag. Errors in bomb impact point will be related to errors in altitude, airspeed, and other aircraft states at the weapon release point. In the analysis to follow, the variation in aerodynamic drag will be ignored.

Let the reference condition of the aircraft at pickle point be defined by pitch angle θ_o, angle-of-attack α, velocity V_o and zero yaw and roll angles. At the point of release the bomb has the same velocity as the airplane. The free fall of the bomb is computed in a reference frame fixed to earth. It is therefore necessary to convert the airplane velocity from the stability axis system to the earth fixed frame. Figure 1 shows this reference frame and also the stability axis system in its reference orientation (note that stability axis is fixed to the aircraft).

Let V be the actual velocity of the airplane, $\alpha_o + \Delta\alpha$ the angle-of-attack and β the sideslip angle. Then the aircraft velocity in the perturbed position of the stability axis system is [1]

$$V_s = \begin{bmatrix} V \cos\beta \cos(\Delta\alpha) \\ V \sin\beta \\ V \cos\beta \sin(\Delta\alpha) \end{bmatrix} \tag{1}$$

The velocity is now transformed to the reference orientation of the stability axis system. If φ, θ and ψ are roll, pitch and yaw angles of the aircraft, then the velocity can be transformed from the perturbed to the reference orientation of the stability axis system by the matrix transformation,

$$L_{vs} = \begin{bmatrix} \cos\psi\cos\theta & -\sin\psi\cos\varphi + \cos\psi\sin\theta\sin\varphi & \sin\psi\sin\varphi + \cos\psi\sin\theta\cos\varphi \\ \sin\psi\cos\theta & \cos\psi\cos\varphi + \sin\psi\sin\theta\sin\varphi & -\cos\psi\sin\varphi + \sin\psi\sin\theta\cos\varphi \\ -\sin\theta & \cos\theta\sin\varphi & \cos\theta\cos\varphi \end{bmatrix} \tag{2}$$

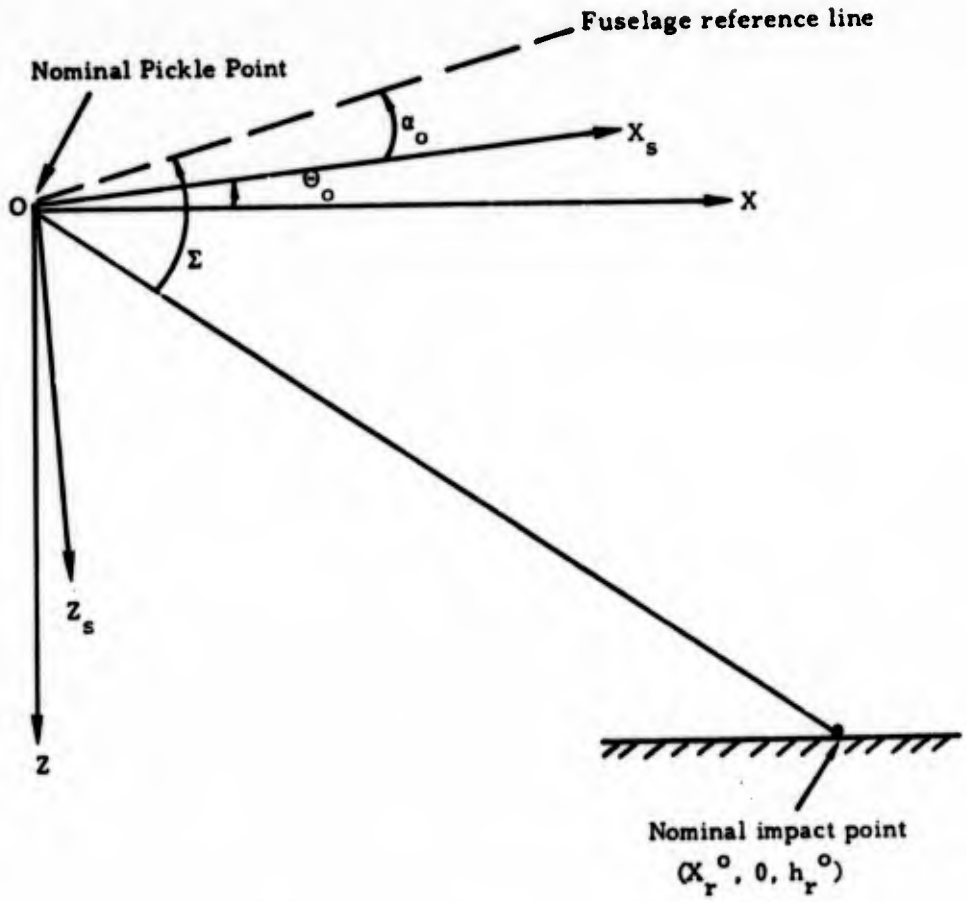

Figure 1 Earth fixed reference system (XYZ) and stability axis system in its reference orientation (X_s Y_s Z_s)

(Origin of coordinate systems at nominal pickle point; Y, Y_s point out of the paper at O)

The velocity can be transformed from the reference orientation of the stability axis sytem to the earth fixed coordinate system by the transformation

$$L_{ev} = \begin{bmatrix} \cos\Theta_o & 0 & \sin\Theta_o \\ 0 & 1 & 0 \\ -\sin\Theta_o & 0 & \cos\Theta_o \end{bmatrix} \qquad (3)$$

The velocity of the perturbed aircraft represented in the earth fixed axis system is, therefore,

$$V_e = L_{ev} L_{vs} V_s \tag{4}$$

The general expression for this is given in Table 1.

Table 1 Coordinate transformation from perturbed stability axis system to earth fixed axis system

$$V_x = V\{\text{Cos } \psi \cos\theta \cos\beta \cos(\Delta\alpha) + \sin\beta (\cos\psi \sin\theta \sin\varphi - \sin\psi \cos\varphi) + \cos\beta \sin(\Delta\alpha) (\sin\psi \sin\varphi + \cos\psi \sin\theta \cos\varphi)\} \cos(\Theta_o) + V\{-\sin\theta \cos\beta \cos(\Delta\alpha) + \cos\theta \sin\varphi \sin\beta + \cos\theta \cos\varphi \cos\beta \sin(\Delta\alpha)\} \sin(\Theta_o)$$

$$V_y = V \sin\psi \cos\theta \cos\beta \cos(\Delta\alpha) + V(\cos\psi \cos\varphi + \sin\psi \sin\theta \sin\varphi) \sin\beta + V(-\cos\psi \sin\varphi + \sin\theta \sin\psi \cos\varphi) \cos\beta \sin(\Delta\alpha)$$

$$V_z = -V\{\cos\psi \cos\theta \cos\beta \cos(\Delta\alpha) + \sin\beta (\cos\psi \sin\theta \sin\varphi - \sin\psi \cos\varphi) + \cos\beta \sin\Delta\alpha (\sin\psi \sin\varphi + \cos\psi \cos\varphi \sin\theta)\} \sin\Theta_o + V\{-\sin\theta \cos\beta \cos\Delta\alpha + \cos\theta \sin\varphi \sin\beta + \cos\theta \cos\varphi \cos\beta \sin\Delta\alpha\} \cos\Theta_o$$

Free Fall of the Bomb

In the nominal condition when the bomb is released at pickle point

$$V_e^o = \begin{bmatrix} V_o \cos\Theta_o \\ 0 \\ V_o \sin\Theta_o \end{bmatrix} \triangleq \begin{pmatrix} V_x^o \\ V_y^o \\ V_z^o \end{pmatrix} \tag{5}$$

The time taken for the bomb to reach the ground after release is

$$T_f^o = \frac{\sqrt{V_z^{o2} + 2gh_r^o}}{g} - \frac{V_z^o}{g} \tag{6}$$

The nominal longitudinal range is

$$X_r^o = V_x^o T_f^o = \frac{V_o \cos \Theta_o}{g} \left\{ \sqrt{V_o^2 \sin^2 \Theta_o + 2gh_r^o} - V_o \sin \Theta_o \right\} \tag{7}$$

and the nominal lateral range is zero.

If the bomb is actually released at (x, y, h) with velocity components (V_x, V_y, V_z), the time to reach the ground is

$$T_f = \frac{\sqrt{V_z^2 + 2(h_r^o - h)\, g} - V_z}{g} \tag{8}$$

The longitudinal range is

$$X_r = x + V_x T_f \tag{9}$$

and the lateral range is

$$Y_r = y + V_y T_f \tag{10}$$

The actual range can be determined by using velocity components from Table 1. For small α, β, φ, θ, ψ and small pertubation in speed, errors in forward and cross range can be simplified. The aircraft velocity in earth fixed reference axis is, approximately,

$$V_e \triangleq V_e^o + \Delta V_e \simeq \begin{bmatrix} V_o \cos\Theta_o + V_o(\Delta\alpha-\theta)\sin\Theta_o + \Delta V \cos\Theta_o \\ V_o\,(\psi+\beta) \\ V_o \sin\Theta_o + V_o\,(\Delta\alpha-\theta)\cos\Theta_o + \Delta V \sin\Theta_o \end{bmatrix} \quad (11)$$

The error in the time to reach the ground is

$$\Delta T_f \simeq \left\{ \frac{V_z^o}{\sqrt{V_z^{o2} + 2h_r^o g}} - 1 \right\} \frac{\Delta V_z}{g} - \frac{h}{\sqrt{V_z^{o2} + 2h_r^o g}}$$

$$= \frac{T_f^o \Delta V_z - h}{\sqrt{V_z^{o2} + 2h_r^o g}} \quad (12)$$

The error in longitudinal range is

$$\Delta X_r = x + \Delta V_x T_f^o + V_x^o \Delta T_f$$

$$= x + V_o\,(\Delta\alpha-\theta)\sin(\Theta_o - \alpha_o)\,T_f^o + \Delta V \cos(\Theta_o - \alpha_o) T_f^o$$

$$+ \frac{V_x^o \left\{ -h + T_f^o\,(V_o\,(\Delta\alpha - \theta)\cos\Theta_o + \Delta V \sin\Theta_o) \right\}}{\sqrt{V_z^{o2} + 2h_r^o g}}$$

$$= x - \frac{hV_x^o}{\sqrt{V_z^{o2} + 2h_r^o g}} + \left\{ V_o \sin\Theta_o\, T_f^o + \frac{V_o \cos\Theta_o\, T_f^o\, V_x^o}{\sqrt{V_z^{o2} + 2h_r^o g}} \right\} (\Delta\alpha-\theta)$$

$$+ \left\{ \cos\Theta_o + \frac{\sin\Theta_o\, V_x^o}{\sqrt{V_z^{o2} + 2h_r^o g}} \right\} \Delta V\, T_f^o \quad (13)$$

$$\triangleq C \begin{bmatrix} x \\ h \\ \Delta\alpha \\ \theta \\ \Delta V \end{bmatrix} \tag{14}$$

$$(\Delta X_r)^2 = C \begin{bmatrix} x \\ h \\ \Delta\alpha \\ \theta \\ \Delta V \end{bmatrix} [x, h, \Delta\alpha, \theta, \Delta V]\, C^T \tag{15}$$

If the initial condition is a random vector, we can compute the variance of the miss distance

$$E(\Delta X_r)^2 = C\chi C^T \tag{16}$$

where,

$$\chi = E \begin{bmatrix} x \\ h \\ \Delta\alpha \\ \theta \\ \Delta V \end{bmatrix} [x, h, \Delta\alpha, \theta, \Delta V] \tag{17}$$

and $E(\Delta X_r)^2$ is the expected value of $(\Delta X_r)^2$; the error in lateral range is

$$\Delta Y_r = y + V_y T_f^o$$

$$= y + (\psi + \beta) V_o T_f^o \tag{18}$$

Its variance can be computed as for the longitudinal system.

Pipper Position at Release

In the nominal flight condition, the pipper is on target with the airplane at the pickle point. Therefore, the correct pipper depression below the fuselage reference line is

$$\Sigma = \tan^{-1}\left(\frac{h_r^o}{X_r^o}\right) - \alpha_o - \theta_o \tag{19}$$

or $$h_r^o = X_r^o \tan(\Sigma - \Theta_o - \alpha_o) \tag{20}$$

A unit vector from the point the bomb is dropped to the reference impact point can be represented in the reference orientation of the stability axis sytem as,

$$\hat{r} = \frac{1}{\ell}\begin{bmatrix} (X_r^o - x)\cos(\Theta_o) - (h_r^o - h)\sin(\Theta_o) \\ y \\ (X_r^o - x)\sin(\Theta_o) + (h_r^o - h)\cos(\Theta_o) \end{bmatrix} \tag{21}$$

$$\ell^2 = (X_r^o - x)^2 + (h_r^o - h)^2 + y^2 \tag{22}$$

This unit vector is for small x, y, and h

$$\hat{r} = \begin{bmatrix} \cos\left\{\Theta_o + \tan^{-1}\left(\frac{h_r^o - h}{X_r^o - x}\right)\right\} \\ \frac{y}{\sqrt{(X_r^o - x)^2 + (h_r^o - h)^2}} \\ \sin\left\{\Theta_o + \tan^{-1}\left(\frac{h_r^o - h}{X_r^o - x}\right)\right\} \end{bmatrix} \tag{23}$$

This unit vector in the perturbed stability axis sytem is given in Table 2. For small error in aircraft states and bomb release point, the error in pipper location is

$$\varepsilon_p^{\text{lateral}} = -\psi \cos(\Sigma - \alpha_o) + \varphi \sin(\Sigma - \alpha_o)$$

$$+ \frac{y}{X_{r_o}} \cos(\Sigma - \Theta_o - \alpha_o) \tag{24}$$

$$\varepsilon_p^{\text{long.}} = \theta + \frac{x h_r^{o} - h X_r^{o}}{h_r^{o2} + X_r^{o2}} \tag{25}$$

Equations (24) and (25) can be solved for x and y. This can be used to remove x and y dependence from Eqs. (13) and (18), if desired.

Table 2 Unit vector along line-of-sight in the perturbed stability axis system

$$\begin{bmatrix} r_x \\ r_y \\ r_z \end{bmatrix} = \begin{bmatrix} \cos\theta\cos\psi\cos\left(\Theta_o + \tan^{-1}\left(\frac{h_r^{o} - h}{X_r^{o} - x}\right)\right) - \sin\theta\sin\left(\Theta_o + \tan^{-1}\left(\frac{h_r^{o} - h}{X_r^{o} - x}\right)\right) \\ \quad + \cos\theta\sin\psi \dfrac{y}{\sqrt{(X_r^{o} - x)^2 + (h_r^{o} - h)^2}} \\ (\sin\varphi\sin\theta\cos\psi - \cos\varphi\sin\psi)\cos\left(\Theta_o + \tan^{-1}\left(\frac{h_r^{o} - h}{X_r^{o} - x}\right)\right) + \sin\varphi\cos\theta\sin\left(\Theta_o + \tan^{-1}\left(\frac{h_r^{o} - h}{X_r^{o} - x}\right)\right) \\ \quad + (\sin\varphi\sin\theta\sin\psi + \cos\varphi\cos\psi) \dfrac{y}{\sqrt{(X_r^{o} - x)^2 + (h_r^{o} - h)^2}} \\ (\cos\varphi\sin\theta\cos\psi + \sin\varphi\sin\psi)\cos\left(\Theta_o + \tan^{-1}\left(\frac{h_r^{o} - h}{X_r^{o} - x}\right)\right) + \cos\varphi\cos\theta\sin\left(\Theta_o + \tan^{-1}\left(\frac{h_r^{o} - h}{X_r^{o} - x}\right)\right) \\ \quad + (\cos\varphi\sin\theta\sin\psi - \sin\varphi\cos\psi) \dfrac{y}{\sqrt{(X_r^{o} - x)^2 + (h_r^{o} - h)^2}} \end{bmatrix}$$

Pre-Weapon Release (Controlled Flight)

The pre-weapon release portion of the RPV attack phase starts at launch with the beginning of dive and ends with weapon release at the pickle point. During this portion of flight, the remote pilot has control over the motions of the aircraft. He must provide an open-loop learned input command so that the RPV follows the predetermined flight path and in addition perform a tracking task so that the RPV follows this desired flight path as closely as possible in the presence of various disturbances. There are four principal sources of errors, which cause deviations in aircraft states from the nominal values at pickle point. They are:

1. Initial Condition Errors. Errors in dive angle, altitude, downrange, airspeed, etc., at initiation of dive.

2. Control Input Errors: Human operator errors in implementing the learned nominal control profile (human motor noise), errors in command transmission (uplink), bias in stick, etc.

3. Tracking Errors. Errors due to longitudinal, lateral and vertical gusts and errors in perception of various displays by the human pilot.

4. System Errors. Signal jamming, loss of instrument, differences in weight and other characteristics of the RPV, etc.

The dive usually is a low angle-of-attack, low speed flight where the assumption of longitudinal-lateral decoupling is valid. Thus, it is possible to use two separate equations for the aircraft motions: one for the longitudinal direction and the other for the lateral direction. Starting from a certain initial condition (or its statistical distribution) at the initiation of dive, the deviation in aircraft states from nominal caused by the errors given above are predicted as the aircraft progresses with the dive. This is called error propagation. Since the disturbances act randomly, this procedure gives a statistical distribution of deviation of aircraft states at any point along the dive and in particular at the

pickle point. The errors at pickle point can be used to predict impact errors according to Eqs. (16) and (17). The error propagation techniques are similar for both longitudinal and lateral directions. We discuss here the longitudinal case.

CONTROLLER/RPV INTERFACE CONSIDERATIONS

Figure 2 shows a schematic diagram of the closed-loop system consisting of the remote human controller and the RPV. The linearized equations governing the longitudinal motions (perturbation from nominal) of an RPV are

$$\dot{x} = Ax + bu + \Gamma w \tag{26}$$

where

$x = [\Delta V, \theta, q, \Delta\alpha, h]$, state vector

$u = \delta e$, elevator input

and $w = (\omega_x, \omega_z, u_n)$

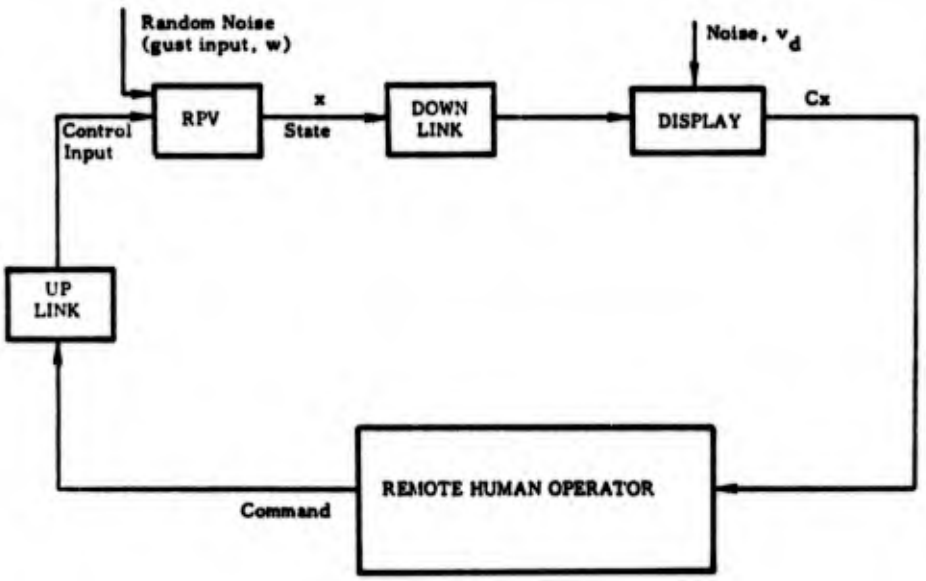

Figure 2 General configuration of an RPV system
(for small perturbations from nominal)

where ω_x and ω_z are windspeed gusts in longitudinal and vertical directions and u_n is the noise in control input (motor noise). The forms of A, b, and Γ are given in [1]. The wind velocity in the longitudinal and vertical directions is assumed to be white with power spectral density W. The remote human controller tries to keep the deviations from nominal path as small as he can using feedback control u.

Certain linear combinations of state variables are measured and transmitted by a downlink to a remote control station. They are displayed to the pilot either using conventional aircraft instruments or an integrated display. There is noise in the measurement of state variables onboard the aircraft and additional noise is added during downlink transmission and display. Let this noise be "white" with covariance R_d. The displayed variables can be represented as

$$z = Cx + v_d \tag{27}$$

Because of basic human limitations and interinstrument scanning, the pilot perceives noisy z, i.e., if y is the perceived signal

$$y = z + v_y = Cx + v_d + v_y \tag{28}$$

where v_y is white observation noise with covariance R_y. It is reasonable to assume that v_d and v_y are independent. Therefore, we can write

$$y = Cx + v \tag{29}$$

$$\begin{aligned} \text{cov}(v) &= (R_d + R_y) \\ &\triangleq R \end{aligned} \tag{30}$$

Notice that we have assumed continuous measurements. If the measurements are discrete, they can be converted into equivalent continuous measurements as explained by Bryson and Ho [2].

ERROR PROPAGATION UNDER NOMINAL CONDITIONS

The effects of the errors mentioned above at the weapon release point are analyzed for a highly skilled and experienced pilot. It is assumed that such a human controller can construct the optimal state estimate from measurements for nominal process and measurement noise and then use a linear combination of these estimated states for feedback (Figure 3). The particular linear combination is such that it minimizes a quadratic function of state deviations and control inputs.

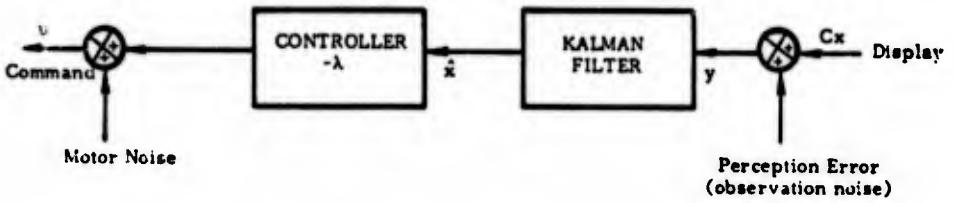

Figure 3 Remote pilot model

Note that the discussion here deals with perturbations from nominal. The states do not include the nominal trajectory. Similarly, the control inputs only represent the corrective part of the control action and exclude the pre-cognitive open-loop nominal command. The optimum filter is

$$\dot{\hat{x}} = A\hat{x} + bu + K\nu \qquad \hat{x}(0) = \hat{x}_o \tag{31}$$

$$\nu = y - C\hat{x} \tag{32}$$

$$K = PC^T R^{-1} \tag{33}$$

$$\dot{P} = AP + PA^T + \Gamma W \Gamma^T - PC^T R^{-1} CP \qquad P(0) = P_o \tag{34}$$

where $\hat{x}_o$ is the best estimate of the initial condition and P_o is the corresponding covariance. Since the filter is optimal, the separation theorem can be used to design the feedback control law assuming that the remote controller minimizes a quadratic performance index of the type

$$J = x^T(T)\, S_f x(T) + \int_0^T (x^T Q x + g u^2)dt \tag{35}$$

which gives the feedback control law

$$u = -\frac{1}{g} b^T S\hat{x} \triangleq -\lambda\hat{x} \tag{36}$$

where S follows the differential equation

$$\begin{aligned} \dot{S} &= -SA - A^T S - Q + S\,\frac{bb^T}{g}\,S \\ S(T) &= S_f \end{aligned} \tag{37}$$

Using the above approach, the filter and controller gains are time varying. Usually, the steady state assumption is made by assuming that T is large. Then Eqs. (34) and (37) become algebraic equations in P and S

$$AP + PA^T + \Gamma W \Gamma^T - PC^T R^{-1} CP = 0 \tag{38}$$

$$SA + A^T S + Q - \frac{Sbb^T S}{g} = 0 \tag{39}$$

Once the controller and filter are designed, the steady state covariance of x can be determined as follows:

Let

$$\begin{aligned} E(xx^T) &= X \\ E(\hat{x}\hat{x}^T) &= \hat{X} \end{aligned} \tag{40}$$

Then, if the filter is optimal

$$X = \hat{X} + P \tag{41}$$

P is obtained from (38) and $\hat{X}$ follows the differential equation

$$\dot{\hat{X}} = (A-b\lambda)\hat{X} + \hat{X}(A-b\lambda)^T + KRK^T \tag{42}$$

which, in steady state, becomes,

$$(A-b\lambda)\hat{X} + \hat{X}(A-b\lambda)^T + KRK^T = 0 \tag{43}$$

ERROR PROPAGATION UNDER DEGRADED CONDITIONS

The above equations give the mean square deviations of the RPV states from nominal when there is no jamming of remote signals and where the parameters of the remote controller, the system and gust, are at the nominal values. If this is not so, the above equations may have to be modified.

To analyze the effects of jamming and degradation in pilot and system performance, it is assumed that the dive phase is so short that the pilot's transfer function as a multiinput/multioutput controller remains fixed and the pilot is not adaptive. In other words, the pilot does not obtain the best state estimates from the measurements. Therefore, the state estimate and state estimation error are not independent and it is necessary to propagate the governing equations simultaneously. We consider the error propagation method for signal jamming and other off-design conditions separately.

Downlink Signal Jamming

With downlink signal jamming, the measurements are available to the pilot intermittently. The control will be poorer than before. To simplify the analysis, it is assumed that blackouts are of constant durations and occur periodically. Let T_1 be the duration during which the signal is received and T_2 the blackout duration (Figure 4). Two assumptions can be made regarding pilot behavior during blackouts leading to two different representations.

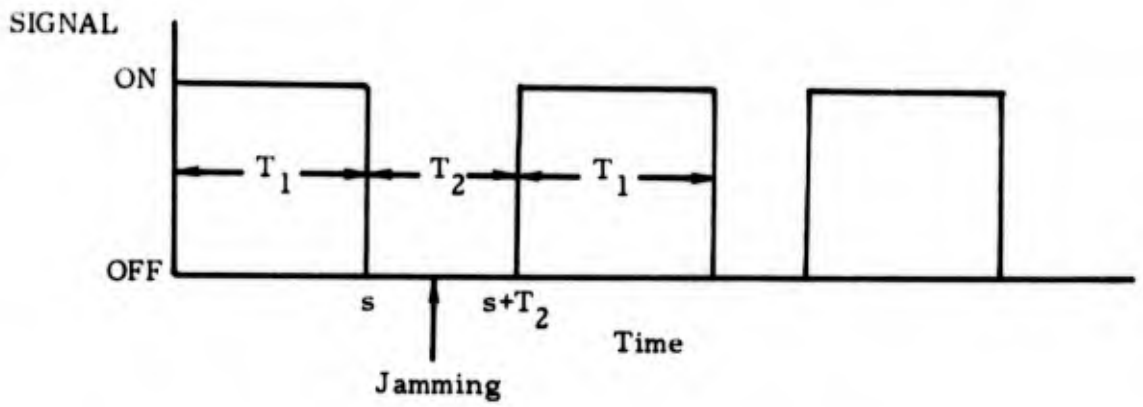

Figure 4 Model of downlink signal jamming

No Feedback During Blackout

Here it is assumed that the pilot is capable of predicting aircraft response for a short period of time after the signal is lost but during a major portion of the blackout he cannot predict aircraft states. To simplify the computation, the pilot is assumed to use open-loop nominal command inputs but not perturbation inputs during the entire blackout period. This leads to the following mathematical model for error propagation during the blackout and signal periods.

- Blackout Period ($s \leq t \leq s+T_2$)

Let blackout start at time s. Let the covariance of x be X. Since there is no feedback perturbation control, u is zero. Equation (26) can be used directly to predict the covariance of x.

$$\dot{X} = AX + XA^T + \Gamma W \Gamma^T \qquad s \leq t \leq s + T_2 \qquad (44)$$

$$X(s) = \text{given}$$

- Signal Period ($s+T_2 \leq t \leq s+T_1+T_2$)

During the blackout period, the human operator does not do any prediction. Therefore, his best estimate of aircraft states at any time is zero. Thus, when the signal is received again

$$\hat{x}(s+T_2) = 0$$

$$\hat{X}(s+T_2) = 0 \tag{45}$$

Therefore, from Eq. (41)

$$P(s+T_2) = X(s+T_2) = \text{given from Eq. (44)} \tag{46}$$

It is assumed that the operator model parameters do not change even when there are periodic blackouts. In other words, filter and controller gains are constant. As a result, the filter representing the human operator as an estimator is not optimal. Therefore, the state estimate and state estimation errors are correlated. The equations governing x and $\hat{x}$ are

$$\frac{d}{dt}\begin{pmatrix} x \\ \hat{x} \end{pmatrix} = \begin{pmatrix} A & -b\lambda \\ KC & A-b\lambda-KC \end{pmatrix}\begin{pmatrix} x \\ \hat{x} \end{pmatrix} + \begin{pmatrix} \Gamma & 0 \\ 0 & K \end{pmatrix}\begin{pmatrix} w \\ v \end{pmatrix} \tag{47}$$

$$s+T_2 \leq t \leq s+T_1+T_2$$

If

$$X^* = E\begin{pmatrix} x \\ \hat{x} \end{pmatrix}(x^T \quad \hat{x}^T) \tag{48}$$

and

$$F^* = \begin{pmatrix} A & -b\lambda \\ KC & A-b\lambda-KC \end{pmatrix}$$

then,

$$\dot{X}^* = F^*X^* + X^*F^{*T} + \begin{pmatrix} \Gamma W \Gamma^T & 0 \\ 0 & KRK^T \end{pmatrix} \tag{49}$$

where

$$X^*(s+T_2) = \begin{pmatrix} X(s+T_2) & 0 \\ 0 & 0 \end{pmatrix} \tag{50}$$

Prediction and Feedback During Blackout

The human operator predicts aircraft states throughout the blackout period starting from his best estimate when the signal is lost and applies the feedback control $-\lambda\hat{x}$. Then the following pilot model is valid.

- Blackout Period ($s \leq t \leq s+T_2$)

Since the human operator uses straight prediction, the filter gains K are zero. The covariance of the estimated state follows the equation

$$\dot{\hat{X}} = (A-b\lambda)\hat{X} + \hat{X}(A-b\lambda)^T \qquad s \leq t \leq s+T_2 \tag{51}$$

$\hat{X}(s)$ given

Also, the prediction error covariance follows Eq. (34) (with K zero)

$$\dot{P} = AP + PA^T + \Gamma W \Gamma^T \qquad s \leq t \leq s+T_2 \tag{52}$$

P(s) given

The covariance of x is

$$X = \hat{X} + P \tag{53}$$

- Signal Period ($s+T_2 \leq t \leq s+T_1+T_2$)

Again, the filter is nonoptimal. Therefore, Eq. (49) with proper initial condition must be used to predict state covariance during the time the signal is being received.

Deterioration in System or Human Performance

If the human controller is not adaptive, i.e., the feedback control gains and the filter gains remain constant, for changes in gusts, control input error and measurement error, the filter and the controller represented by the human pilot will not be optimal. Then, the assumption of decoupling between the controller and the filter is not valid. The coupled Eq. (49) with proper initial conditions must be propagated to obtain time varying or steady state covariance.

ANALYTICAL PREDICTION OF PERFORMANCE DECREMENTS FOR THE XQM-103 DUE TO SYSTEM OR HUMAN CONTROLLER DEGRADATIONS

Using the technique described above, predictions are made on the effect of various parameters on performance decrements. The performance here is measured in terms of the miss distance at the bomb impact point.

Nominal Condition

The XQM-103 is used as the baseline RPV. The longitudinal stability and control coefficients are assumed to remain constant during the dive. The longitudinal equations of motion for this RPV are [3] (altitude 5,000 ft. and Mach no. 0.5); units: ft., radian, sec.

$$\frac{d}{dt}\begin{bmatrix}\Delta V\\ \theta\\ q\\ \Delta\alpha\\ h\end{bmatrix} = \begin{bmatrix}-.05513 & -32.21 & 0 & 21.9 & 0.0\\ 0.0 & 0.0 & 1.0 & 0.0 & 0.0\\ -.000337 & 0.0 & -.8472 & -27.68 & 0.0\\ -.00021 & 0.0 & .99 & -2.644 & 0.0\\ 0.0 & 548.2 & 0.0 & -548.2 & 0.0\end{bmatrix}\begin{bmatrix}\Delta V\\ \theta\\ q\\ \Delta\alpha\\ h\end{bmatrix}$$

$$+\begin{bmatrix}0.0\\ 0.0\\ -10.60\\ .002\\ 0.0\end{bmatrix}\delta e + \begin{bmatrix}-.005512 & -.0188 & 0.0\\ 0.0 & 0.0 & 0.0\\ -.000337 & -.0505 & -10.6\\ -.00021 & -.00482 & .002\\ 0.0 & 0.0 & 0.0\end{bmatrix}\begin{bmatrix}\omega_x\\ \omega_z\\ u_n\end{bmatrix} \qquad (54)$$

where ω_x, ω_z are windspeeds in longitudinal and vertical directions and u_n is the motor noise in input δe.

The pickle point is at 548.2 ft sec^{-1} speed, 2000 ft. altitude and -15^o flight path angle. Nominal time for the bomb to reach the ground is, using Eq. (6),

$$T_f^o = 7.58 \text{ sec.} \qquad (55)$$

and the nominal downrange at pickle point is

$$X_r^o = 4{,}013 \text{ feet} \qquad (56)$$

During the controlled flight, the pilot uses displays of airplane speed, angle-of-attack, pitch angle and altitude. The root-mean-square errors (observation noise) in perceiving airplane speed, angle-of-attack, pitch angle and altitude have nominal values of 8 ft sec^{-1}, 1^o, 2^o, and 100 ft, respectively, and the sampling time is .5 sec (which means that the pilot looks at these instruments twice every second on the average). The power spectral density matrix of the measurement noise is*

$$R = \text{diag}[64,\ 3.0 \times 10^{-4},\ 1.2 \times 10^{-3},\ 10^4] \qquad (57)$$

Horizontal and vertical gusts have rms values of 25 ft sec^{-1} and 8 ft sec^{-1}, respectively, with correlation time 0.5 sec. Human motor noise enters the controls as random errors with rms value of .3 deg and correlation time .5 sec.* The power spectral density matrix, W, is

$$W = \text{diag}[625,\ 70,\ 2.6 \times 10^{-5}] \tag{58}$$

Error Propagation During the Post-Weapon Release Phase

Equation (13) can be used for the nominal aircraft dive parameters at pickle point to predict bomb impact errors (miss distance) in terms of deviations in aircraft states from nominal values at pickle point. For the XQM-103 RPV under the conditions given above, this would give

$$\Delta X_r = x - 1.372h + 6.582 \times 10^3(\Delta\alpha - \theta) + 10.04\,\Delta V \tag{59}$$

Also, the error in pipper position at pickle point is (Eq. (25))

$$\varepsilon_p^{long} = \theta + .26x - .97h \tag{60}$$

Error Propagation During the Pre-Weapon Release Phase

To analytically predict the effect of jamming and other decrements in system and human operator performance, the techniques of the previous section are used for error propagation considering the system degradations, one at a time. As mentioned before, the human operator model is considered nonadaptive, which may be an oversimplistic assumption in some cases.

---

*The power spectral density is computed using the approximation that noise correlation time is much smaller than the system characteristic time. Then, after Bryson [2]

Power spectral density = 2x (correlation time) x (mean square value)

Initial Condition Errors

The remote pilot is considered to be an optimal filter followed by a quadratic cost controller. Based on the state Eqs. (54) and noise statistics in Eqs. (57) and (58), an optimal filter is designed for which the gains are shown in Table 3. The feedback control law is designed based on minimizing a cost function which is quadratic in state and control variables. It is assumed that the pilot uses a tight control law to the point where additional effort by him does not decrease RMS state deviations significantly. The weights in the quadratic cost are chosen accordingly. The quadratic cost is

$$J = \int_0^T \left| 10(\Delta V)^2 + 4.33 \times 10^4 \left((\Delta\alpha)^2 + 1.88h^2 + 10^6 (\delta e)^2 \right| \right| dt \qquad (61)$$

same as equation (65), page 36

The resulting control gains are shown in Table 3.

Table 3 Filter and controller gains

Filter

$$K = \begin{bmatrix} .14361288 & -36.82874700 & 4.22500529 & -.00308958 \\ -.00017263 & 1.97997667 & .50713700 & .00000833 \\ -.00024945 & 2.47886469 & 2.10833866 & .00001638 \\ .00007922 & 2.02854799 & .74899420 & -.00000449 \\ -.48274693 & 277.61608600 & -37.4322460 & .10040878 \end{bmatrix}$$

Controller

$$\lambda = (-.00000942 \quad 1.37574420 \quad .11888664 \quad -1.21168680 \quad .00137113)$$

The effect of initial conditions at initiation of dive on the RPV state at pickle point are determined by the eigenvalues and eigenvectors of the filter and controller (the eigenvalue of the closed-loop system are the sum of eigenvalues of the controller and the filter). All eigenvalues are well damped (Table 4) and only the eigenvalue for the control of aircraft speed is small (with a corresponding large time constant). Aircraft speed can be controlled by changing the throttle which we have not considered here. The effect of initial conditions, therefore, should be insignificant at the pickle point.

Signal Jamming

System performance is predicted for the case in which there is intermittent jamming of the downlink signal. It is assumed that the loss of signal occurs at periodic intervals and that the human operator uses no feedback signal during the blackout period.

Figure 5 shows the increase in RMS miss distance, $\sqrt{(\Delta X_r)^2}$, for various levels of signal jamming and for two values of the duration of the lost signal. The x-axis measures $T_2/(T_1+T_2)$, which is the fraction of total time the signal is off and the ordinate is the RMS miss distance. Zero intercept on the x-axis corresponds to nominal conditions and the intercept one corresponds to the case where the downlink is jammed throughout the dive and only prelearned control signal is applied.

The initial condition is assumed to correspond to the statistical steady state with no signal jamming. In practical terms, this implies that the RPV had been flying for some time with insignificant signal jamming prior to initiation of dive. The two curves in the figure correspond to the cases in which the signal is off periodically for a period of either 1 sec or 2 sec. For up to 25% signal jamming, there is insignificant decrease in pilot performance and bomb impact accuracy. If the signal is lost for more than half the time, the increase in miss distance is quite serious. Note that the analysis here does not include bias in pilot control inputs. This error will further degrade the performance.

Table 4 Eigenvalues of controller and filter

Controller

Complex Eigenvalue (1)	Complex Eigenvector (1)
-1.770 + 5.16i	-.046 - .037i
	-.019 - .002i
	.049 - .096i
	-.016 - .012i
	1.000 + .000i
Complex Eigenvalue (2)	**Complex Eigenvector (2)**
-.610 + .587i	-.056 - .006i
	-.001 + .000i
	.000 - .000i
	.000 - .000i
	1.000 + .000i
Real Eigenvalue (1)	**Real Eigenvector (1)**
-.053 + .000i	-.987
	.000
	-.000
	.000
	-.155

Filter

Complex Eigenvalue (1)	Complex Eigenvector (1)
-2.987 + 5.641i	-.061 + .028i
	-.006 - .016i
	.100 - .029i
	.002 - .019i
	1.000 + .000i
Complex Eigenvalue (2)	**Complex Eigenvector (2)**
-.227 + .046i	-.012 - .038i
	-.000 + .000i
	-.000 + .000i
	.000 - .000i
	1.000 + .000i
Real Eigenvalue (1)	**Real Eigenvector (1)**
-.089 + .000i	.027
	-.000
	-.000
	.000
	.999

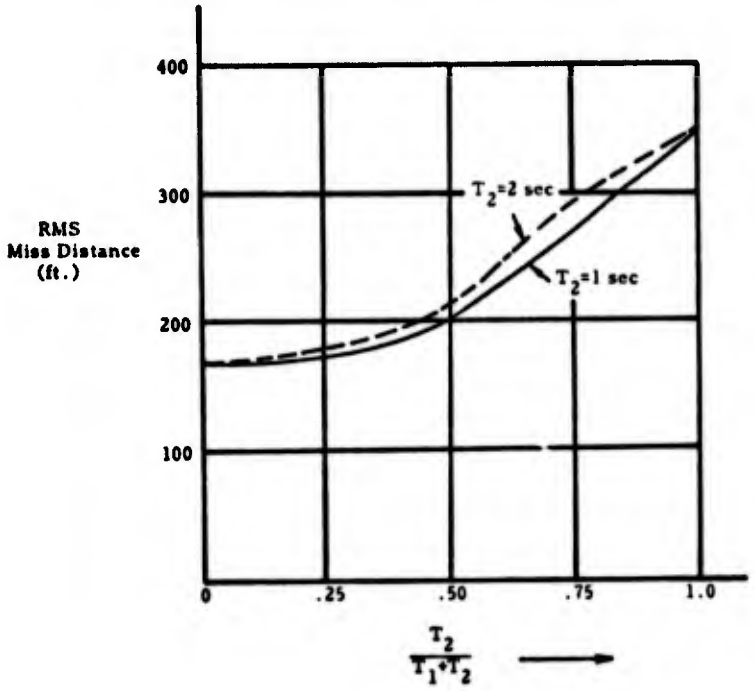

Figure 5 Miss distance errors with signal jamming

Control Input Error

Figure 6 shows the effect of changes in random noise in control inputs because of human motor noise and noise in signal uplink. The x-axis shows the RMS control input error and the y-axis gives the standard deviation of miss distance. The errors are quite serious beyond the nominal value of 0.3^{o} RMS.

Human Perception Error

Increased noise in downlink signal channel because of bad weather or other reasons can degrade signal information about the state of the RPV. This can lead to a decrement in the performance of the pilot even if he were adaptive. As before, we assume that the pilot is not adaptive. The miss distance as a function of the increase in perception error covariance is shown in Figure 7. The miss distance increases steadily with increase in error covariance, but does not show a drastic increase for the changes considered (as the control input error does). A fourfold increase in perception error covariance leads to approximately a 50% increase in miss distance.

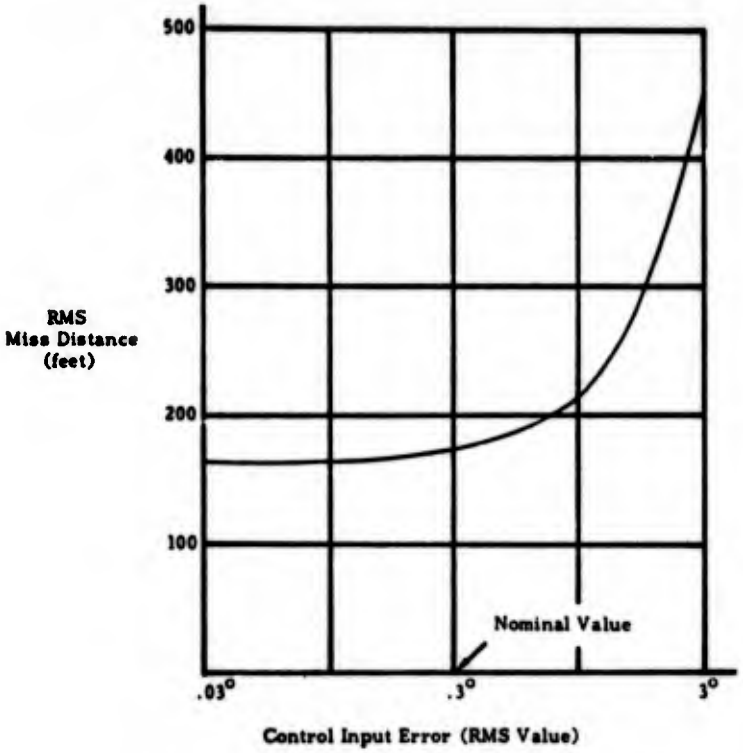

Figure 6 Effect of degradation in control input errors (motor noise) on impact errors

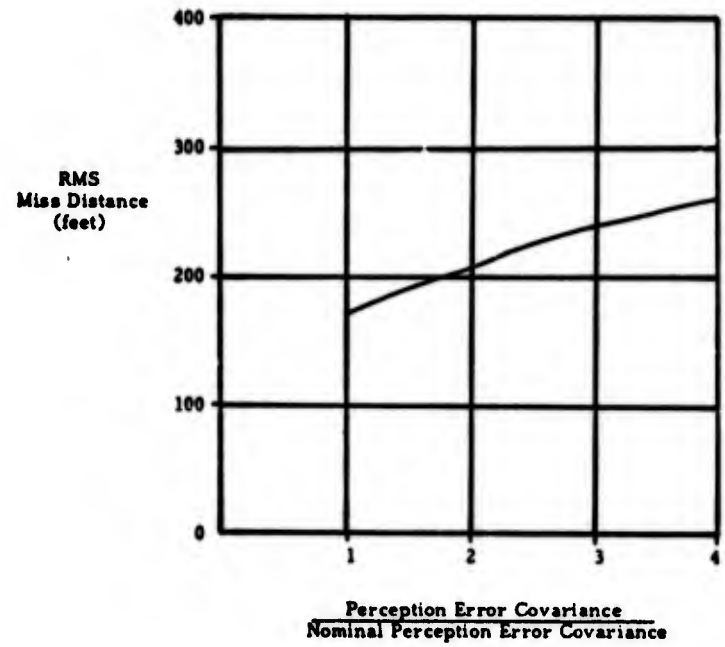

Figure 7 Miss distance as a function of perception error covariance

To study the effect of errors in single measurement, the covariances of perception errors in velocity, pitch angle and height are increased tenfold, one at a time. The comparison in Table 5 shows that the increase in perception error of pitch angle is most critical.

Table 5 Effect of degradation in human perception on impact error

10 X Increase in Covariance of Perception Error In	Impact Error (feet)
Velocity	178
Pitch Angle	209
Height	189
Nominal	173

ANALYSIS OF TAKEOFF AND LANDING PHASES

The takeoff and landing are two other critical tasks in an RPV mission. The takeoff phase involves taxiing in the terminal, starting and accelerating on the runway, leaving the runway, climbout and finally approach to the cruise mode. The landing phase requires approach, glideslope following, touchdown, deceleration on the ground and taxiing to the hangar area. The difference between the takeoff and landing phases and the weapon delivery phase is that the former are usually to be carried out close to the base airstrip in a "friendly" environment while the latter is over enemy territory.

With a relatively short experience, a remote pilot should be able to perform ground taxiing so that the RPV follows a desired path on the ground and does not either go off the taxiway or collide with other taxiing or parked RPV's. This would, of course, require a ground traffic controller or some coordination between the remote pilots of different RPV's.

In the climb section of the takeoff phase, it is important to ensure that the remote operator maintains RPV speed above stall and the vehicle follows a predetermined flight path which would depend upon the surrounding terrain and the presence of other approaching and departing aircraft and RPVs. Following such a flight path would require nominal (precognitive) elevator, aileron, and rudder inputs. The level of traffic in the terminal airspace would dictate how closely the nominal flight path has to be followed.

The landing phase starts with airport location and approach to the glide-slope path. The RPV loses altitude and groundspeed during the approach phase, so that at the beginning of glideslope, the aircraft speed is close to the landing speed. Again, the RPV must follow the nominal trajectory maintaining speed above stall. The remote pilot should initiate the flare just prior to touchdown. These maneuvers may have to be carried out under IFR conditions and in gusty winds.

The errors which force the RPV away from the nominal three-dimensional flight path during launch and landing are similar to the weapon delivery phase. However, since these phases are performed closer to the remote pilot over a "friendly" territory, the initial condition, control input, and tracking errors are typically smaller than for weapon delivery. There is usually no jamming of uplink or downlink signals and the airplane is much cleaner and lighter during landing (because of no external stores and reduced fuel weight). In addition, better ground instrumentation at the airstrip would provide the remote pilot with an improved estimate of the aircraft orientation and speed. These factors should provide the remote pilot with better handling of the RPV trajectory in the terminal airspace.

The technique of performing the RPV analysis is the same for the takeoff phase as for the landing phase. The landing phase is more important since the touchdown should occur within a certain longitudinal and lateral distance from the nominal position of the touchdown point and with a reasonable sink rate. Also, the longitudinal and lateral speeds should not deviate too much from the nominal. It should be noted, however, that much higher errors are permissible in an RPV than in a piloted aircraft because there is no human being onboard.

The performance of the remote RPV pilot will be evaluated in the presence of errors mentioned above for the longitudinal motions during the landing phase. As in the weapon delivery phase, it is assumed that the pilot is highly skilled, motivated and experienced, in that he behaves like an optimal filter followed by a controller, based on optimized quadratic loss function (see Figure 3). The nominal path is assumed prespecified and the pilot is able to reproduce the precognitive inputs exactly.

AIRCRAFT EQUATIONS OF MOTION AND NOMINAL CONDITIONS

XQM-103 is again used as the baseline RPV. The longitudinal equations of motion at 5000 ft. altitude and Mach number 0.3 are [3] (in units of feet, radian, seconds)

$$\frac{d}{dt}\begin{bmatrix}\Delta V\\ \theta\\ q\\ \Delta\alpha\\ h\end{bmatrix} = \begin{bmatrix}-.03774 & -32.2 & 0.0 & 9.709\\ 0.0 & 0.0 & 1.0 & 0.0\\ -.000026 & 0.0 & -.4959 & -8.798\\ -.00065 & 0.0 & .99 & -1.568\\ 0.0 & 305.5 & 0.0 & 305.5\end{bmatrix}\begin{bmatrix}\Delta V\\ \theta\\ q\\ \Delta\alpha\\ h\end{bmatrix}$$

$$+\begin{bmatrix}0.0\\ 0.0\\ -10.66\\ .004\\ 0.0\end{bmatrix}\delta e + \begin{bmatrix}-.03774 & -.0749 & 0.0\\ 0.0 & 0.0 & 0.0\\ -.000026 & -.02933 & -10.66\\ -.00065 & -.00523 & .004\\ 0.0 & 0.0 & 0.0\end{bmatrix}\begin{bmatrix}\omega_x\\ \omega_y\\ u_n\end{bmatrix} \qquad (62)$$

where the symbols have the same meanings as before. The root-mean-square errors in perceiving RPV longitudinal speed, pitch angle, angle-of-attack and altitude have nominal values of 4 ft sec^{-1}, $.5^o$, $.5^o$, and 10 feet, respectively, and the samping time is 0.5 sec, the same as in the weapon delivery phase. The power spectral density of the measurement noise is

$$R = \text{diag}[16,\ 7.5 \times 10^{-4},\ 7.5 \times 10^{-4},\ 10^2] \qquad (63)$$

Notice that in this case, a much improved measurement of altitude is available because the aircraft is much closer to the ground. The horizontal and vertical gusts are random and have RMS values of 17 ft sec^{-1} and 5 ft sec^{-1}. The control input errors are $.1^o$ RMS, again with a correlation time of .5 sec. The power spectral density matrix of the process noise is, therefore,

$$W = [280,\ 25,\ 3.0 \times 10^{-6}] \qquad (64)$$

Using the state Eqs. (62) and process and measurement noise covariance matrices (63) and (64), a filter is designed to estimate aircraft states. Table 6 shows the filter gains and the eigenvalues and eigenvectors of the filter. Then a linear feedback law is determined by optimizing the following quadratic performance index.

$$J = \int_0^T \{10(\Delta V)^2 + 4.33 \times 10^4(\theta^2+(\Delta\alpha)^2) + 1.88h^2+10^4\delta e^2\}dt \qquad (65)$$

The resulting control gains and the eigenvalues/eigenvectors of the closed-loop system are given in Table 7. All eigenvalues are well damped and have small time constants. This represents good response for initial condition errors.

The root-mean-square errors are evaluated at the touchdown point for the RPV/pilot model given above. The steady state assumption is made so that Eqs. (38) and (39) can be used to determine these errors. Table 8 shows the RMS errors in velocity, pitch angle, angle-of-attack, flight path angle and height. The errors in velocity and height look quite reasonable. The RMS error in flight path angle is 1.20°. The pilot may have to use terminal control to reduce deviations in flight path angle. The error of 7.56 feet in height will reflect as an error in the position of the touchdown point. If the glide path angle is 2° at touchdown, the RMS error in the touchdown point is 216 feet.

The remote pilot performance can be evaluated under degraded conditions during landing and takeoff as in the weapon delivery phase.

Table 6 RPV remote pilot filter gains and characteristic values for landing

Gains

$$K = \begin{bmatrix} .125 & -64.72 & 53.36 & -.0037 \\ -.000303 & 2.22 & 1.76 & .000198 \\ 0.0 & 4.05 & 9.19 & -.000169 \\ .000250 & 1.76 & 3.74 & .000132 \\ -.0234 & 263.6 & 176.2 & .355 \end{bmatrix}$$

Eigenvalues and Eigenvectors

Eigenvalue	$-3.50 \pm 3.83i$	-.915	-.104	-.354
Eigenvector	$-.124 \mp .128i$	-.784	-.979	0.0
	$-.0033 \pm .0237i$	.0135	-.0011	0.0
	$-.125 \mp .0115i$	.0115	-.0015	0.0
	$-.0230 \pm .0202i$	-.0025	.00026	0.0
	1.0	-.621	-.204	1.0

Table 7 RPV remote pilot controller gains and characteristic values for landing

Gains

$\lambda = (-.00392, 2.64, .776, .962, .0137)$

Eigenvalues and Eigenvectors

Eigenvalue	$-3.46 \pm 4.80i$	-2.63	-.0547	-.765
Eigenvector	$-.0325 \pm .0084i$	0.0	.966	-.995
	$-.0043 \pm .0081i$	0.0	0.0	-.0173
	$-.0238 \mp .0486i$	0.0	0.0	.0133
	$-.007 \pm .0077i$	0.0	0.0	.0171
	1.0	1.0	.260	.0937

All in units of ft, radian, sec.

Table 8 Root-mean-square RPV state deviations at touchdown

State	ΔV	θ	$\Delta\alpha$	$\Delta\gamma$	h
Units	ft sec^{-1}	deg	deg	deg	ft
RMS Deviation	4.19	1.30	1.36	1.20	7.56

ERROR PROPAGATION TECHNIQUE AS A TOOL IN RPV ANALYSIS AND DESIGN

In the last sections, it was shown how the methods of error covariance propagation could be used to predict human performance under normal and degraded conditions. The technique is very powerful and could prove useful in the design and analysis of various sytems and subsystems, in the pilot/vehicle interactions and also in training remote RPV pilots.

Certain assumptions are made regarding the methods used by remote controllers in flying the RPVs. Pilot performance can be evaluated under different pilot models (e.g., different set of assumptions to model his control actions), which are within the capabilities of a trained human being. The models could include simplified compensators with optimized pole-zero locations or some selected nonlinearities in place of the optimal control models. This can be used to determine the smallest order of the compensator, whose performance is close to the optimal control model. It seems reasonable that the remote pilot would choose this compensator, since a high order transfer function involves more integrators and is harder to implement by the remote pilot. These models can be verified by experiment. Once the desired pilot model is discovered, pilot training programs could be designed to help pilots "learn" this model.

Error propagation methods can be used to evaluate the displays and instrumentation. For example, it may be necessary to decide whether the conventional instruments are sufficient or an integrated display is required. Each set of instruments and display techniques has a certain measurement error associated with it. If the desired RPV performance is specified for various missions, it is possible to choose those displays which will meet the mission requirements even under moderately degraded conditions. This could also be used to evaluate errors in the downlink channel. The control sticks in the remote pilot cockpit and the noise in uplink for command transmission can also be designed using the error covariance propagation. The tolerable stick errors and human motor noise errors can be specified. This would also establish the kind of missions that a remote pilot can perform using an RPV.

CONCLUSIONS AND RECOMMENDATIONS

The error covariance propagation methods are useful in predicting RPV/remote pilot performance for the baseline system and under degraded conditions. The covariance propagation was carried out for the weapon delivery phase and the takeoff/landing phases. These techniques circumvent the need for expensive Monte Carlo simulations in establishing subsystem specifications and RPV capabilities during different missions.

For the weapon delivery phase, the performance was determined in terms of the miss distance of the bomb from the target under normal and degraded conditions. This specifies the tolerable extent of downlink signal jamming and loss in signal quality because of bad weather, poor transmission and reception, etc. A study was made of the effect of human controller motor noise on the miss distance and it is shown that beyond a certain point this error caused serious degradation in performance. Many more studies need to be carried out in a similar fashion before the system requirements during this phase are determined.

In this effort, the miss distance is determined for bombs released at zero relative speed from the RPV and have no guidance after release. A similar analysis can be performed for the missiles which are fired from the RPV and have either autonomous guidance or remote guidance from the RPV through a telemetry system. The equations of motion are different, though the technique is the same. The use of error propagation methods for the takeoff and landing is also demonstrated. A similar analysis as for the weapon delivery phase can be performed.

Much further research is required in developing the error propagation methods as a quick design tool for the RPV systems and in developing training programs for RPV pilots. The following are some of the recommendations for future work.

1. Carry out the analysis for various pilot models, both adaptive and nonadaptive, linear and nonlinear. Then one could choose a feasible pilot model which provides the best performance. The feasible models

are such that pilots can learn them through training. Devise pilot training programs so that they learn to be the desired form of the controllers. The model that a pilot represents can be determined and verified by experiments.

2. Consider errors other than "white" noise. There are possibly biases and scale factor errors in instruments and in the control stick and rudder pedals. There are possible delays in various parts of the system.

3. Consider changes in RPV characteristics like weight, unsymmetrical loading (because of external stores), center of gravity location, etc.

4. Study the differences in performance of remote and onboard pilots and in their control techniques. This would help design remote pilot "cockpit".

5. Consider multiRPV control by remote pilots (i.e., the possibility of one pilot flying several RPV's.

REFERENCES

1. Etkin, B., Dynamics of Atmospheric Flight, John Wiley and Sons, New York, 1972.

2. Bryson, A.E. and Ho, Y.C., Applied Optimal Control, Ginn Blaisdell, Waltham, 1969.

3. Day, C.N., "Stability and Control Derivatives for the XQM-103 RPV," Private Communications, Aerospace Medical Research Laboratory, Wright-Patterson AFB, Ohio 45433, December 1973.

4. Rankine, Jr., R.R., The Effects of Aircraft Dynamics and Pilot Performance on Tactical Weapon Delivery Accuracy, School of Engineering and Applied Science, University of California, Los Angeles, November 1970.

5. Kleinman, D.L. and Killingsworth, W.R., A Predictive Pilot Model for STOL Aircraft Landing, Final Report to NASA Langley Research Center, Contract NAS1-11727, October 1973.

APPENDIX 1

DESIGN OF A COMMAND DIRECTOR FOR THE RPV WEAPON DELIVERY TASK

The purpose of this appendix is to present an approach to the design of a control command director for manual air-to-ground weapon delivery on an RPV strike mission. As discussed in THE MANUAL WEAPON DELIVERY TASK, fully manual weapon delivery requires that the human operator fly the RPV along a prescribed (learned nominal path) trajectory from launch to weapon release. The human operator must perform the three main tasks of: (1) decision to initiate attack, (2) generation of open-loop (learned) command inputs to the aircraft, and (3) tracking to minimize the effects of gust disturbances on the nominal weapon delivery profile. The approach to command director design discussed in the following pages is based on providing decision and command aids to simplify the first two tasks. Task 1 is simplified by giving the pilot a range reticle command where the decision to attack is made when the target, as seen on the TV monitor, coincides with the crosshairs of the range reticle image. The generation of open-loop command inputs by the pilot is aided by converting the feedforward task to a commanded path-following task. In effect, the reticle displacement can be dynamically programmed to reflect the desired line-of-sight commands corresponding to the desired nominal flight profile.

As noted earlier, the TV camera onboard the RPV is assumed to have a line-of-sight (LOS) that is a fixed angle below the fuselage reference line (FRL). The control center displays to the remote pilot are assumed to be airspeed, attitude, altitude, angle-of-attack, sideslip angle and a TV monitor with a programmable reticle image. In addition, it is assumed that using appropriate algorithms (e.g., wind estimation), true airspeed, groundspeed, and flight path angle can be computed.

Figure A.1 shows a sample nominal trajectory, KLMP, that the RPV is required to follow. L is the launch point, P is the pickle point and M stands for the point of transition from line-of-sight tracking over LM to tracking a dynamically compensated reticle over MP. The proposed algorithm consists of two parts: (a) line-of-sight tracking with a fixed reticle image (called a range reticle) dis-

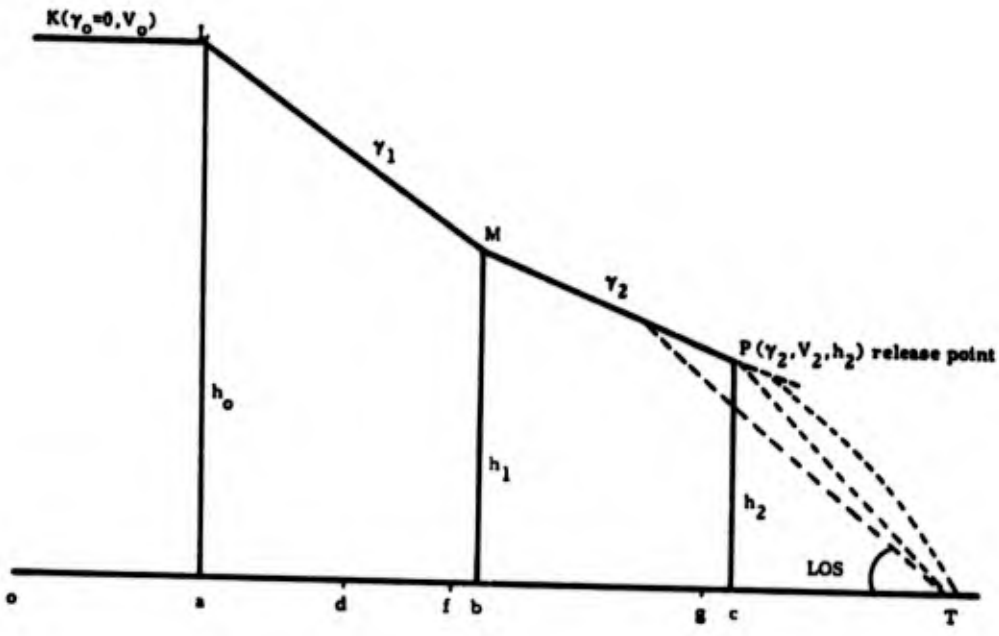

Figure A.1 Nominal trajectory for RPV dive bombing

play, and (b) tracking a trajectory with a flight path angle γ_2 with a dynamically compensated reticle image display (called a command reticle).

The range reticle is displayed to the pilot during the phase KLM. It's location on the TV screen is fixed at a precomputed position so that the target T would lie exactly under the range reticle when the aircraft is at launch point L with an altitude h_o and range aT. Thus, the operator must initiate attack at point L by tracking the target T with the range reticle over path LM. The line-of-sight tracking mode over path LM can be effectively used to obtain a continuous on-line range estimate by using the relation

$$r(t) = \frac{h(t)}{\tan \gamma_1(t)} \qquad (A.1)$$

where h(t) is the altitude and $\gamma_1(t)$ is the flight path angle over LM. Since h and γ_1 are assumed to be measured (or computed), estimation techniques can be applied to determine $\hat{r}(t)$ along LM. When the variance of the range estimator falls below a certain threshold (to be defined or determined experimentally) at some point d in ab, then range estimation can be terminated and the best estimate $\hat{r}(d)$ used thereafter as a reference marker.

The purpose of the command reticle is to aid the pilot in flying a flight profile MP to the bomb release point P with aircraft velocity V_2, flight path angle γ_2 and altitude h_2. For simplicity, it is assumed that the pilot sets the throttle to achieve aircraft velocity V_o at P and does not change it subsequently. Velocity V_o must be chosen such that the release flight condition (V_2, h_2, γ_2) can be met by flying the nominal path LMP. The following cues must be provided to the remote operator.

1. When to switch from FPA γ_1 to γ_2;

2. Command reticle to help him track a path MP (or FPA γ_2); and

3. When to initiate weapon release.

The first cue requires that a lead signal be given to the human operator at some point f prior to approaching transition point b. Selection of a point f can be carried out as follows.

Along leg ab, the range estimator is assumed to give the best range estimate $\hat{r}$ at point d. The following computations must be carried out once:

$$(1) \quad cT = V_{2x} t_{cT} = \frac{V_2 \cos \gamma_2}{g} \left(V_2 \sin \gamma_2 + \sqrt{V_2^2 \sin^2 \gamma_2 + 2gh_2} \right) \qquad (A.2)$$

(2) Assume time to travel bc is t_{bc} seconds; then,

$$bc = (V_2 \cos \gamma_2) t_{bc} \quad \text{and,}$$

$$h_1 = h_2 + bc \tan \gamma_2 \qquad (A.3)$$

$$= h_2 + V_2 t_{bc} \sin \gamma_2$$

Thus, switch point (b,M) can be determined using either h_1 or bT where,

$$bT = bc + cT \qquad (A.4)$$

(3) Range to target is determined by the equation

$$r = r(d) - \int_{t_d}^{t} V_i \cos \gamma_i \, dt \qquad \text{(A.5)}$$

where $i = \begin{cases} 1 \text{ (leg ab)} \\ 2 \text{ (leg bc)} \end{cases}$

(4) To ensure that the switchover takes place smoothly, introduce a lead time

$$T_L = \frac{\Delta\gamma}{2\dot{\gamma}} = \frac{(\gamma_1 - \gamma_2)}{2\dot{\gamma}}$$

$$\dot{\gamma} = (\text{normal acceleration/horizontal velocity}) = \frac{ng}{V_1 \cos \gamma_1}$$

$n = .2$ for comfort (~ 6 ft./sec^2)

This can be much higher for an RPV, $n = 8$ (say). Note that at high G's, T_L becomes small

$$T_L = \frac{(\gamma_1 - \gamma_2)\ (V_1 \cos \gamma_1)}{2ng}$$

$$r_L \begin{matrix} \text{horizontal} \\ \text{range} \\ \text{lead} \end{matrix} = fb = (V_1 \cos \gamma_1)\, T_L = \frac{(\gamma_1 - \gamma_2)\ (V_1 \cos \gamma_1)^2}{2ng}$$

Therefore, a new flight path angle command λ_3 must be initiated at point f when the range given by Eq. (3) equals (r_L + bT) where bT is given in Eq. (2).

Now the pilot must be aided in flying an FPA of γ_2 and keeping the target in sight; this is done by generating a reticle whose LOS will remain on target provided the pilot flys at λ_2--the vehicle depression angle LOS is given by the relation

$$\tan(\text{LOS}) = r/h_c$$

At every instant of time r is computed from Eq. (3) and h_c is given by

$$h_c = (r-cT) \tan \gamma_2 + h_2$$

Lead time can be introduced into the command vehicle to take care of pilot response delays.

Finally, an indication of release time or pickle point P must be given to the pilot. Clearly, the release instant is when $r = cT$. If the pilot response delay is T_p, then a release light should be activated when the measured altitude is $h = h_2 + (V_2 \sin \gamma_2)T_p$.

Several modifications can be added to this proposed algorithm. For example, it is quite easy to display to the remote pilot a continuous prediction of the bomb impact point using covariance propagation techniques outlined in the text of this report. Such a display can, in effect, provide the human controller with continuous status information on the effectiveness of his overall weapon delivery strategy. Another use of this algorithm and display would be as a training tool for novice remote controllers, whereby a given nominal control strategy can be taught to new operators with a minimum of time and effort.